NUMERICAL COMPUTATION OF THE INDUCED CURRENTS IN A 3-DIMENSIONAL HEAD MODEL DUE TO TMS

N. S. Hassan[1], D. Sami[2], M. E. Rasmy[3]
[1]Department of Biomedical Engineering, Cairo University, Giza, Egypt
[2]Dept of Biomedical Engineering, Misr University for Science and Technology, Sixth of October City, Egypt
[3] Biomedical Engineering, Cairo University, Giza, Egypt

***Abstract*-Transcranial magnetic stimulation (TMS) is considered a promising non-invasive, painless therapeutic tool in psychiatry and a diagnostic tool in neurology. The main motivation of this study was to use the finite element method to compute the detailed magnitude and spatial distribution of the currents induced in a realistic 3D head model, based on MRI, by TMS. Asymmetries in the electrical properties and the coil placement, with respect to different brain tissues, influenced the magnitude of the induced current throughout the brain significantly. The maximum induced currents were observed in the cerebral spinal fluid (CSF) where the conductivity was the greatest. The current vector distribution showed circulating fields affecting the facial muscles under one of the stimulating coils. In addition, a gradual decrease in the induced current was observed as the current circulates farther from the coils in each of the brain transverse planes. However, major exceptions were detected at the grooves (fissures and sulci) where the induced current follows tortuous pathways and gradually increases.**

***Keywords*-current density, finite element model, transcranial magnetic stimulation.**

I. INTRODUCTION

Interest in transcranial magnetic stimulation (TMS) has been driven by its successful application in the treatment of serious psychological disorders such as depression and schizophrenia. Brain stimulation with TMS is achieved by placing a figure of eight coils on the head and magnetically inducing electric currents in different brain tissues. To date, most of the effort has focused on the attempt to stimulate localized neurons deep in the brain. However, the actual measurement and the precise prediction of the induced currents and its distribution in specific territories in the brain is still a very complicated task and necessitate the computation of these currents via numerical techniques. Several numerical models based on infinite half plane and perfect spheres have been developed to provide insights on the current distribution in homogeneous biological tissues [1-6]. Results of these models indicated that the induced currents parallel to the skin are the main factors influencing nerve fiber stimulation. However, this conclusion is the result of the simplified nature of the geometries used in these models. Other studies based on inhomogeneous models, were developed to account for tissue heterogeneity [7-9]. Results showed that induced current distribution was influenced by the interface between tissue boundaries. Moreover, Nadeem, Thorlin, Ghandi and Persson computed the induced currents on a cross section of a multi-tissue brain model [10]. The results indicated the presence of localized hot spots under the center of the stimulating coils. Subsequently, Wagner, Zahn, Grodzinsky and Leone generated a realistic head model that accounts for changes in tissue electrical properties [11]. Using a head model with five dissimilar structures they showed that the tissue boundaries have a major effect on the induced currents. While these results provided insights into the currents generated by TMS, the computation of these currents in more realistic geometries with multi-structures located deeper in the brain and having a greater level of detail (such as sulci) is still lacking. The specific goal of this study is to use the finite element (FE) method to compute the detailed description and quantification of the magnitude and spatial distribution of the induced currents in a more anatomically faithful TMS head model incorporating different head structures.

II. METHODOLOGY

A. Computational method

The time-varying solver module of a commercially available FE software package Maxwell® 3-D Field Simulator (Ansoft Corporation, Pittsburgh, PA) was used to solve Maxwell's equations for computing the magnetic and spatial distribution of the induced electric fields and current density (J) in a 3-D realistic head model due to TMS. The Maxwell 3D solver takes into account the geometry being modeled, electrical and magnetic properties, sources of ac magnetic fields and the appropriate boundary conditions describing the field behavior. The FE method was used to divide the geometry into a mesh consisting of thousands of tetrahedral elements of various sizes. This method is very well suited for accurate modeling of complicated shapes. The technique uses second-order quadratic polynomials to approximate electromagnetic field quantities in each tetrahedral element and computes these quantities by minimizing an energy functional. If the field solution for an element in the mesh is not within a user specified percentage error, the software further subdivides the element into smaller elements and again generates a field solution for these smaller elements. In this manner, the mesh is repeatedly refined until the solution reaches the required accuracy.

B. Head Model

In this paper, we have constructed a new detailed 3-D model to simulate the human head as shown in Fig. 1. A hundred and twenty transverse magnetic resonance imaging (MRI) anatomical slices of a 35 year old male with no neurological abnormalities were segmented, stacked and surface rendered to generate the head model. The head model consisted of ten structures: the skin, skull, cerebral spinal fluid (CSF), gray matter (GM), white matter (WM), ventricles, thalamus, caudate nuclei, cerebellum and medulla

(see Fig. 1). Since the power spectrum of typical simulators is composed of components less than 10 KHz, the conductivities of biological tissues were considered constant and were assigned values given in table I.

C. Transcranial Magnetic Stimulator Model

The Magstim Rapid stimulator applicator 9925 [Wales, UK] was modeled as a figure-eight shaped copper coil with two 34 mm-radius wings. The amplitude of the peak current in the TMS coil is $I = 8 \times 10^3$ A, which is in the range of typical values used in clinical settings. The source coils were placed 7 mm above the head and in a position used clinically for the treatment of depression. Solutions were obtained for the frequency component of the current source set at 10 KHz.

TABLE I
ELECTRICAL PROPERTIES USED FOR DIFFERENT BRAIN STRUCTURES [12], [13]

Tissue	Conductivity (S/m)
Skin	0.0201
Skull	0.0203
Cerebral Spinal Fluid	2.00
Gray Matter	0.107
White Matter	0.065
Ventricles	2.00
Caudate Nuclei	0.107
Thalamus	0.107
Cerebellum	0.127
Medulla	0.107

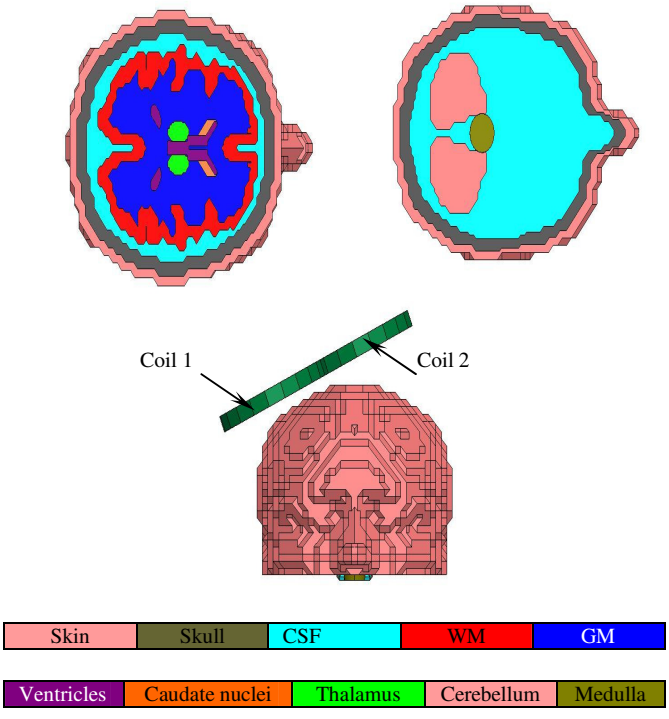

Fig. 1. The modeled geometry. (A) Cut planes throughout the brain to show different brain structures. (B) Simulated figure-eight coil placement above the 3D head model.

III. NUMERICAL RESULTS

The TMS applicator is placed on the surface of the human head model as shown in Fig. 1. The magnitude, spatial distribution and the vector orientation of the induced current density were analyzed in two different transverse planes as shown in Fig. 2. The maximum J was 25 A/m^2 under the center of the coils in the CSF, the tissue with the highest conductivity. In general, the induced J decreases as we move farther from the coils in the left hemisphere as compared to the right hemisphere in the same transverse plane. However, several hot spots in the J were observed under the peripheral sides of the coils indicating that the spatial distribution is highly dependent on the coil placement with respect to different brain tissues. Fig. 2b depicts the J vector circulation in a figure-eight path in a transverse plane where the two brain hemispheres are separated. In addition, deeper structures such as the ventricles, the caudate nuclei and the thalamus exhibited induced currents as high as 13 A/m^2, 1.4 A/m^2 and 1.6 A/m^2 respectively, as compared to a value of 1.25 A/m^2 in the surrounding WM (see Fig. 2c). On the other hand, the J followed tortuous paths in structures located deeper in the brain (see Fig. 2d). The magnitude of the J gradually increases from the posterior end of the groove towards the anterior end (see inset in Fig. 2.b). Fig. 3 shows how the J circulates along the right side of head (facial muscles) due to the effect of the second coil.

Although there is a general consensus that the maximum J decreases away from the coil surface, increased values were observed at some transverse planes in different brain structures (see Fig. 4). For example, the maximum J in the CSF decreased in the superficial planes located at depths of 22 mm to 42 mm below the surface of the coils. Since the area of the head encompassing these planes is small, regions of these planes are located under specific sectors of the coils where the J is known. At a depth of 52 mm where the transverse planes grow wider, some regions become under the peripheral sections of the coils. Thus, these regions are located under coil sections where side peaks in the J are observed causing the maximum J in these planes to increase. Fig. 4 demonstrated these variations in the J in other brain tissues and structures. Due to the large variations in the J data, we have chosen the y-axis scale to be logarithmic. This is a compromise in order to keep the dynamic range in the graph while still being able to observe the region of large J values (i.e. the CSF region).

IV. DISCUSSION AND CONCLUSIONS

We have presented numerical results on the modeling of TMS, based on clinically used applicator parameters, using a realistic 3D head model composed of different structures with different tissue electrical properties.

According to our computations, we confirmed that the induced currents were influenced by the conductivity of the model. These results agreed qualitatively with earlier half plane and experimental studies [8], [5], but now in a multi-tissue model that was more indicative of a true head model. The J induced in the brain exhibited numerous hot spots that can affect the sight and extent of the region being stimulated.

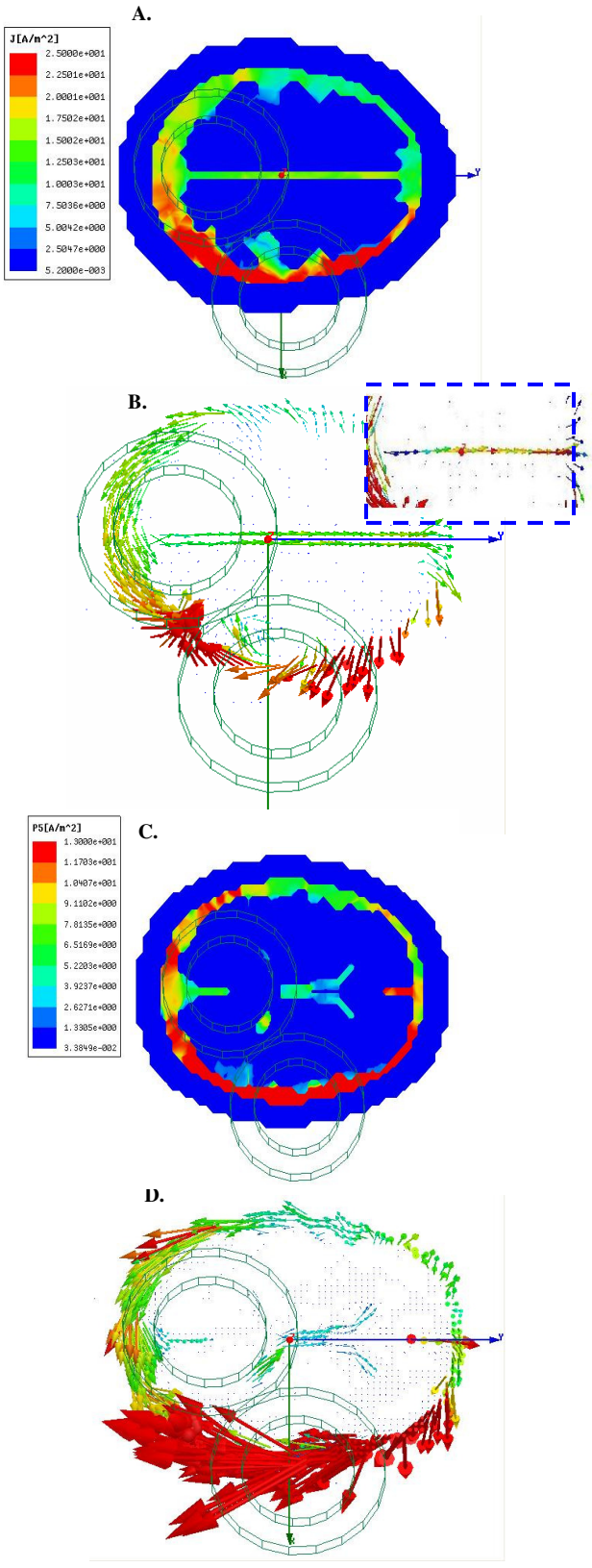

Fig. 2. Current density magnitude and vector plots on two transverse cross sections throughout the brain. (a) Current density magnitude plot on a across section 42 mm below the coils. (b) Induced current vector plot in the same transverse plane as in **a**. (c) Current density magnitude plot on a cross section 62 mm below the coils. (d) Induced current vector plot in the same transverse plane as in **c**. The Inset in b is a magnified view of the J vectors where the scale and number of colors in its pallet were changed to be able to show the gradual change in J.

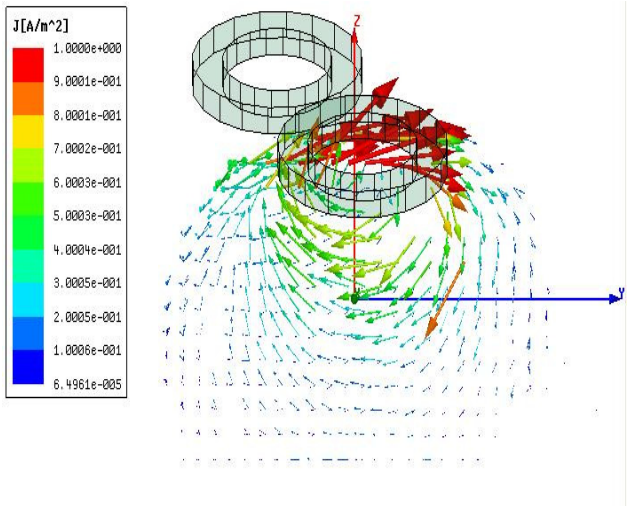

Fig. 3. Induced current vector plot on the surface of the facial muscles on the right side of the head below coil 2.

The location of these hot spots is highly dependant on the head geometry and the relative tissue/structure to coil placement. In addition, significant deviations in the J as compared to homogeneous models were observed in different brain structures. For example, the ventricles, which are filled with CSF, exhibited large values of induced currents as compared to the surrounding WM and GM. Therefore, theories suggesting that the J only activates superficial cortical neurons need to be re-examined. In addition, our model provided means to test the validity of the complaints from patients who experience a tingling sensation in their facial muscles during the TMS sessions (see Fig. 4). Finally, our results demonstrated the complicated pathways the J follows as it passes through grooves (i.e. fissures and sulci) in the brain.

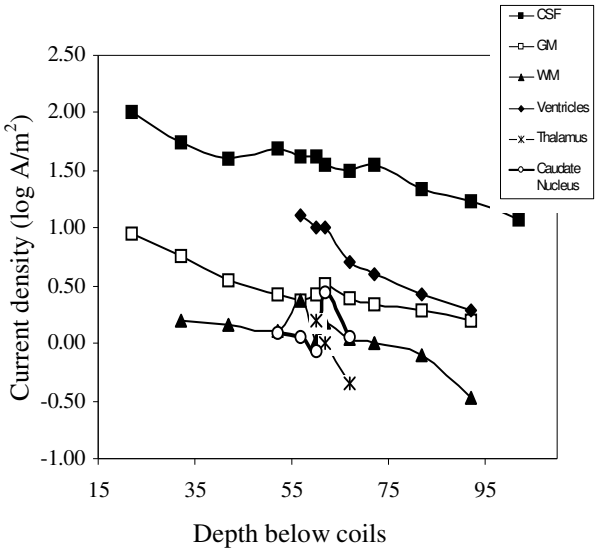

Fig. 4. The maximum J at different depths in different brain structures below the coils. Due to the large variations in the J values, the y-axis scale is not sequential

In this paper, we did not account for the anisotropic nature of brain tissues. However, to some extent anisotropy was considered in the model as the brain was treated as a heterogeneous tissue with varying conductivity.

In conclusion, taking into account the parameters identified as affecting the J magnitude and distribution, our results may have far reaching consequences in providing psychiatrists with a better understanding of the territories stimulated in the brain as well as the degree of excitation during therapy sessions. Our study is aimed to help in refining and designing new noninvasive TMS devices for better localized brain stimulation. Ultimately, we hope to integrate our results with imaging modalities such as PET and fMRI to implement TMS as a profound neural prosthesis.

ACKNOWLEDGMENT

The authors acknowledge the contribution of the Maxwell 3D software from the Ansoft Corporation, Buc, France. We would also like to thank Dr. Nahla Nagy for providing valuable insights into the use of the Magstim applicator in clinical studies and TMS sessions.

REFERENCES

[1] P. S. Tofts, "The distribution of induced currents in magnetic stimulation of the nervous system," *Phys. Med. Biol.*, vol. 35, pp. 1119–1128, 1990.
[2] B. Roth and P. Basser, "A model of stimulation of a nerve fiber by electromagnetic induction," *IEEE Trans. Biomed. Eng.*, vol. 37, pp. 588–597, June 1990.
[3] K. Esselle and M. Stuchly, "Neural stimulation with magnetic fields: Analysis of induced electrical fields," *IEEE Trans. Biomed. Eng.*, vol. 39, pp. 693–700, 1992.
[4] P. J. Basser, "Focal magnetic stimulation of an axon", ," *IEEE Trans. Biomed. Eng, vol. 41,pp. 601-606, 1994.*
[5] H. Eaton, "Electric field induced in a spherical volume conductor from arbitrary coils: Applications to magnetic stimulation and MEG," *Med. Biol. Eng. Comput.*, pp. 433–440, 1992.
[6] D. Cohen and B. N. Cuffin, "Developing a more focal magnetic stimulator. Part 1: Some basic principles," *J. Clin. Neurophysiol.*, vol. 8, pp. 102–111, 1991.
[7] J. M. Saypol, B. J. Roth, L. G. Cohen, and M. Hallett, "A theoretical comparison of electric and magnetic stimulation of the brain," *Ann. Biomed. Eng.*, vol. 19, pp. 317–28, 1991.
[8] R. Liu and S. Ueno, "Calculating the activating function of nerve excitation in inhomogeneous volume conductor during magnetic stimulation using the finite element method," *IEEE Trans. Magn.*, vol. 36, pp. 1796–1799, July 2000.
[9] P. Miranda, M. Hallett and P. J. Basser,"The electric field induced in the brain by magnetic stimulation: A 3-D finite element analysis of the effect tissue heterogenity and anisotropy" *IEEE Trans. Biomed. Eng.*, vol. 50, pp. 1047–1085, 2003.
[10] M. Nadeem, T. Thorlin, O. Gandhi, and M. Persson, "Computation of electric and magnetic stimulation in human head using the 3-D impedance method," *IEEE Trans. Biomed. Eng.*, vol. 50, pp. 900–907, July 2003.
[11] T. Wagner, M. Zahn, A. Grodzinsky, A. Pascual-Leone,"Three-dimensional head model simulation of transcranial magnetic stimulation," *IEEE Trans. Biomed. Eng.*, vol.51, pp. 1586–1598, 2004.
[12] K. R. Foster and H. P. Schwan, "Dielectric properties of tissues," in *Biological Effects of Electromagnetic Fields*, C. Polk and E. Postow, Eds. Boca Raton, FL: CRC Press, 1996, pp. 25–102.
[13] C. Gabriel, S. Gabriel, and E. Courthout, "The dielectric properties of biological tissues: 1. Literature survey," *Phys. Med. Biol.*, vol. 41, pp. 2231–2250, 1996.